JOURNAL OF VIROLOGY, Feb. 2001, p. 2019–2023 Vol. 75, No. 4
0022-538X/01/$04.00+0 DOI: 10.1128/JVI.75.4.2019–2023.2001

Hantavirus Nucleocapsid Protein Oligomerization

AYNA ALFADHLI, ZAC LOVE, BRIAN ARVIDSON, JOSHUA SEEDS, JESSICA WILLEY, AND ERIC BARKLIS*

Vollum Institute and Department of Microbiology, Oregon Health Sciences University, Portland, Oregon 97201-3098

Received 9 August 2000/Accepted 21 November 2000

Hantaviruses are enveloped, negative-strand RNA viruses which can be lethal to humans, causing either a hemorrhagic fever with renal syndrome or a hantaviral pulmonary syndrome. The viral genomes consist of three RNA segments: the L segment encodes the viral polymerase, the M segment encodes the viral surface glycoproteins G1 and G2, and the S segment encodes the nucleocapsid (N) protein. The N protein is a 420- to 430-residue, 50-kDa protein which appears to direct hantavirus assembly, although mechanisms of N protein oligomerization, RNA encapsidation, budding, and release are poorly understood. We have undertaken a biochemical and genetic analysis of N protein oligomerization. Bacterially expressed N proteins were found by gradient fractionation to associate not only as large multimers or aggregates but also as dimers or trimers. Chemical cross-linking of hantavirus particles yielded N protein cross-link products with molecular masses of 140 to 150 kDa, consistent with the size of an N trimer. We also employed a genetic, yeast two-hybrid method for monitoring N protein interactions. Analyses showed that the C-terminal half of the N protein plus the N-terminal 40 residues permitted association with a full-length N protein fusion. These N-terminal 40 residues of seven different hantavirus strains were predicted to form trimeric coiled coils. Our results suggest that coiled-coil motifs contribute to N protein trimerization and that nucleocapsid protein trimers are hantavirus particle assembly intermediates.

Hantaviruses, such as the *Sin Nombre hantavirus* (SNV) and *Prospect Hill virus* (PHV), are members of the bunyavirus class of viruses (3, 20, 24). They are enveloped, negative-strand RNA viruses and carry three genomic RNA segments: the L segment, which encodes an RNA-dependent RNA polymerase; the M segment, which encodes envelope glycoproteins G1 and G2; and the S segment, which encodes the viral nucleocapsid (N) protein (24). Hantaviruses are of medical importance, because many of them cause either a hemorrhagic fever with renal syndrome or a hantaviral pulmonary syndrome, which is characterized by lung damage and cardiac dysfunction (25).

Models for hantavirus replication at the cellular level have been based on direct experiments and by inference from work on other bunyaviruses. The general replication cycle starts with G1 and G2 binding to B3 integrins (7, 8) or other cell surface receptors, followed by virus entry and uncoating. After entry, L protein-mediated primary transcription of mRNAs occurs in the cytoplasm, apparently using an orthomyxovirus-like cap-snatching mechanism (4, 14). Following mRNA translation, transcription shifts from mRNA to cRNA and viral RNA synthesis, and ribonucleoprotein (RNP) structures are formed (4, 14, 24). The RNPs appear to be composed of viral RNAs, N proteins, and presumably L proteins and accumulate on the cytoplasmic sides of cellular membranes, possibly through interactions with the G1 and G2 proteins (9, 21). Evidence suggests that RNPs use microfilaments for transport to virus assembly sites (23) and that, in contrast to other bunyaviruses, hantavirus assembly occurs at the plasma membranes of infected cells (9, 22).

Central to the process of hantavirus assembly are the viral N proteins. The N proteins have been shown to bind viral RNAs in vitro (27)—possibly via the C-terminal 90 to 100 residues (10)—and are likely candidates to bind to the viral glycoproteins during virus assembly or budding. N protein coding regions have been sequenced from a number of hantavirus strains and are well conserved (1, 3, 13, 20, 24, 26, 28; Fig. 1). However, the deduced sequence of the 420- to 430-residue, 50-kDa N protein shows no obvious RNA binding motif (27), has no structurally informative homologs, and does not help explain how N proteins may associate to form virus particles or subviral structures. To examine their structure and function, we initially analyzed the quaternary structure of bacterially expressed, N-terminally His-tagged SNV N proteins. Previous studies showed that such proteins required detergent or chaotropic denaturants for solubilization (5, 27), requiring refolding protocols to achieve native conformations (27). To avoid traditional denaturants, we analyzed N protein solubilization across a panel of buffer conditions (15) and found that His-tagged SNV N proteins were soluble in 500 to 1,000 mM Mg^{2+} ($MgSO_4$ or $MgCl_2$) at neutral pH (pH 6.0 to 8.0; data not shown).

Although N proteins obtained in high magnesium ion conditions were soluble, they could be pelleted by high-speed centrifugation (146,000 × *g*, 1 h), suggesting that they formed multimers or aggregates. Consequently, we examined the aggregation state of N proteins by 15 to 30% sucrose gradient centrifugation. As illustrated in Fig. 2A, most magnesium-solubilized SNV N was found at the bottom of such a gradient (fraction 25), with proteins detectable through fractions 8 to 25. These results suggest that the N proteins formed high-order multimers or aggregates, with a broad range of subunits.

* Corresponding author. Mailing address: Mail Code L220, Vollum Institute and Department of Microbiology, Oregon Health Sciences University, 3181 SW Sam Jackson Park Rd., Portland, OR 97201-3098. Phone: (503) 494-8098. Fax: (503) 494-6862. E-mail: barklis@ohsu.edu.

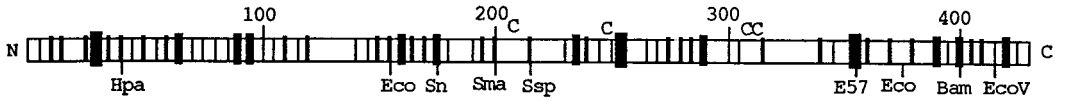


```
  1 MSTLK EVQDN ITLHE QQLVT ARQKL KDAER AVELD PDDVN KSTLQ SRRAA VSALE TKLGE LKREL ADLIA  70
    --Q-R -I-EE --R-- ----I ----- -E--- T--V- ----- ----- ---S- --T-- D--A- F--Q- --V-S
 71 AQKLA SKPVD PTGIE PDDHL KEKSS LRYGN VLDVN SIDLE EPSGQ TADWK SIGLY ILSFA LPIIL KALYM 140
    R--MD E---- ----- L---- --R-- -Q--- ---L- HL-ID --T-- ----L --IV- LT--V V--L- -----
141 LSTRG RQTIK ENKGT RIRFK DDSSY EEVNG IRKPR HLYVS MPTAQ STMKA DEITP GRFRT IACGL FPAQV 210
    -T--- ---T- ----- ----- ----- -D--- --R-K ----- ----- ----- E-L-- ----- -V--- ----I
211 KARNI ISPVM GVIGF SFFVK DWMER IDDFL AARCP FLPEQ KDPRD AALAT.....NRAYF ITRQL QVDES KVSDI
    M---- ----- ----- A---- --ADK VKA-- DQK-- --KAE PR-GQ P-GEAEFLSSI---- MN--A VL--T HLP--
281 EDLIA DARAE SATIF ADIAT PHSVW VFACA PDRCP PTALY VAGMP ELGAF FAILQ DMRNT IMASK SVGTS 350
    DA-VE L-ASG DP-LP DSLEN --AA- ----- ----- --CI- I---A ----- ----- ----- ----- T---A
351 EEKLK KKSAF YQSYL RRTQS MGIQL DQKII ILYMS HWGRE AVNHF HLGDD MDPEL RELAQ TLVDI KVREI 420
    ----- ----- ----- ----- ----- --R-- LM--I E--N- V---- ----- ----- -Q--- A-I-Q --K--
421 SNQEP LKL
    ----- --I
```

FIG. 1. Hantavirus N protein. Shown at the top is the map of the coding region of the N protein of SNV from residues 1 to 428. Vertical lines are indicative of the number of charged residues per five residue segments: thin lines depict one charged residue per segment while progressively thicker lines depict two, three, and four charged residues per segment. Cysteine (C) residues are denoted above the map line, while positions of restriction endonuclease sites in the coding region are shown below the line. Beneath the map, the SNV N protein sequence (3) is provided, along with a comparison to the sequence of PHV (20). Amino acids are depicted in standard single letter code, while restriction enzyme abbreviations are as follows: Hpa, *Hpa*I; Eco, *Eco*RI; Sn, *Sna*B1; Sma, *Sma*I; Ssp, *Ssp*I; E57, *Eco*571; Bam, *Bam*HI; EcoV, *Eco*RV.

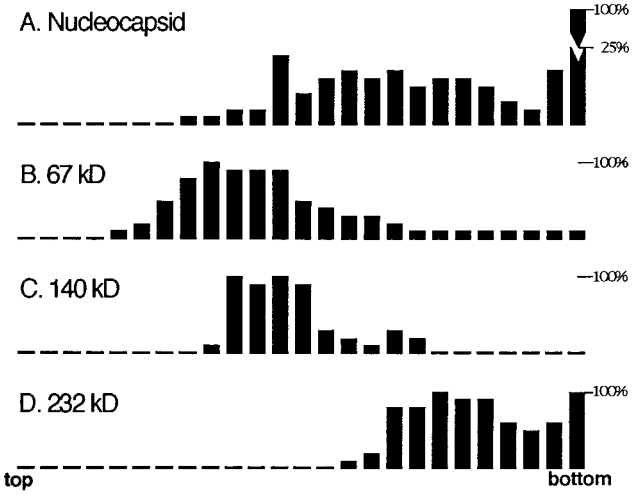

FIG. 2. Sucrose gradient fractionation of hantavirus N proteins. The His-tagged hantavirus (SNV) N protein (5) was expressed in *Escherichia coli* cells, solubilized in 100 mM HEPES (pH 7.0)–1 M $MgSO_4$, and applied to a 15 to 30% sucrose gradient in 50 mM Tris (pH 7.4)–100 mM NaCl–0.1 mM EDTA in parallel with high-molecular-weight marker proteins (Amersham Pharmacia Biotech). Gradients were centrifuged at 4°C at 243,000 × *g* for 18 h, after which 25 0.2-ml fractions were collected from the gradient top to bottom, as indicated. Fractions were separated by sodium dodecyl sulfate-polyacrylamide gel electrophoresis and detected by Coomassie blue staining for markers (19) or by N protein immunoblotting (11, 17, 18), using anti-hantaviral N protein monoclonal antibody Hy11E5EF6CE7 as the primary antibody and an alkaline phosphatase-conjugated secondary antibody. After detection, protein levels were quantitated densitometrically and are displayed as percentages of the highest detected protein level across all gradient fractions for a given protein. Gradient profiles correspond to the SNV N protein (50 kDa) (A), bovine serum albumin (67 kDa) (B), lactate dehydrogenase tetramers (140 kDa) (C), and catalase tetramers (232 kDa) (D).

However, we also observed a small N protein peak halfway through the gradient in fraction 12 (Fig. 2A). When compared with size marker proteins centrifuged in a parallel gradient (Fig. 2B to D), the fraction 12 N protein band appeared to be heavier than bovine serum albumin (67 kDa; Fig. 2B), smaller than catalase tetramers (232 kDa; Fig. 2D), and about the same size as lactate dehydrogenase tetramers (140 kDa; Fig. 2C) (19). These results were repeated on two independent occasions and are consistent with the notion that a small percentage of magnesium-solubilized N proteins were detectable as trimers, which would have a molecular mass of approximately 150 kDa. We believe these putative trimers to be noncovalently associated, as the gradient peak was not readily apparent when magnesium-solubilized N proteins were treated with 0.05% sodium deoxycholate (data not shown).

Although gradient analyses suggested that bacterially expressed N proteins formed trimers and higher-order oligomers, we wished to characterize N protein interactions in hantavirus particles and virus-infected cells. To do so, Vero E6 (African green monkey kidney) cells were infected with the nonpathogenic PHV (20) strain, and cells and released virus particles were collected for analysis. Samples were either mock treated or treated with the membrane-permeable, cysteine-specific cross-linking agent bis-maleimidohexane (BMH; Pierce) (11, 17, 18) prior to electrophoretic fractionation and immunoblot detection of PHV N proteins. As shown in Fig. 3, lane B, BMH cross-linking of particle-associated N proteins yielded a novel band at 146 kDa, compared to those of mock-treated samples (Fig. 3, lane A). Although this band could represent an N protein cross-link to a cell-derived or viral partner with a mass of about 100 kDa, its size is consistent with that of an N protein trimer. If that is the case, it implies that at least two of the five PHV N protein cysteine residues are accessible for reaction with BMH. When the cross-linked products of infected VeroE6 cell samples were analyzed, a band with a calculated mass of 142 kDa was observed (Fig. 3, lane F), suggesting that PHV N proteins trimerize in infected host cells. However, an addi-

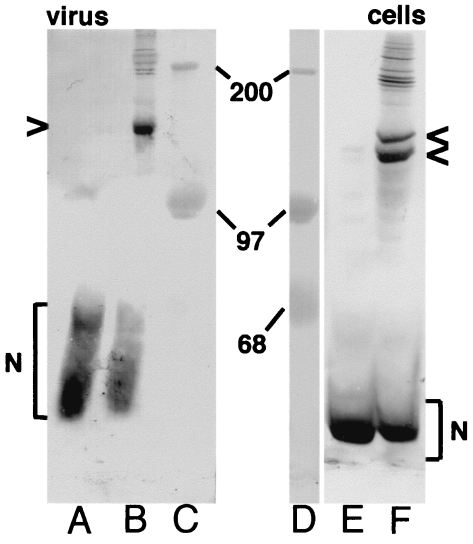

FIG. 3. Cross-linking of hantavirus N proteins. Virus particles (lanes A and B) and cell pellets (lanes E and F) from PHV-infected Vero E6 (African green monkey kidney) cells were collected and either mock treated (lanes A and E) or treated with a 1 mM concentration of the cross-linking agent BMH (11, 17, 18) (lanes B and F). After treatments, samples were fractionated by sodium dodecyl sulfate-polyacrylamide gel electrophoresis along with size markers (lanes C and F), and N proteins were detected by immunoblotting, using the anti-N protein monoclonal antibody Hy12A6CF6 as the primary antibody and an alkaline phosphatase-conjugated anti-mouse secondary antibody (Promega). N protein and 200-, 97-, and 68-kDa size marker bands are as shown. Cross-link products are indicated by arrowheads. The calculated sizes of cross-link products were 146 kDa (lane B), 142 kDa (lane F), and 135 kDa (lane F), while the predicted size of the N protein is 50 kDa.

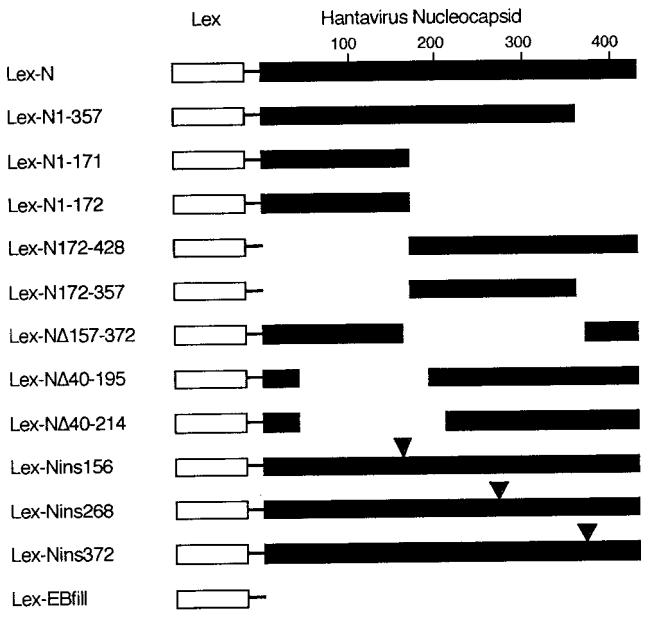

FIG. 4. Recombinant N protein constructs. Shown are maps of the coding regions for LexA-N fusion proteins which were used to assay N protein-protein interactions, in conjunction with a wt SNV N protein (3) fusion to the VP16 (12) transcriptional activation domain. LexA domains are indicated by white boxes, and SNV N protein domains are depicted by black boxes, with amino acid numbers (see Fig. 1) shown at the top. Fusion protein constructs were based on Lex-EBfill, which expresses the DNA binding domain of LexA (2, 6, 12, 16). Lex-N expresses the LexA domain, fused to the full-length, wt N protein coding region. Lex-N1-357, Lex-N1-171, and Lex-N1-172 encode Lex-N fusion proteins, which were truncated after N protein codons 357, 171, and 172, respectively. Lex-N172-428 encodes a fusion protein which has an N-terminal N protein coding region deletion, removing N protein codons 1 to 171. Lex-N172-357 encodes an N protein truncated at its amino (residues 1 to 171) and carboxy (residues 358 to 428) termini. The Lex-NΔ157-372, Lex-NΔ40-195, and LexNΔ40-214 plasmids encode Lex-N proteins with the indicated codon deletions of the N protein, while Lex-Nins156, Lex-Nins268, and Lex-Nins372 have four codon insertions after codons for the indicated amino acid residues. Exact juncture and mutation sequences are available on request.

tional cross-link band at 135 kDa was detected (Fig. 3, lane F). This band could represent a variant form of N protein oligomer or could be an adduct between PHV N protein and either a cellular protein or PHV glycoproteins. Despite these uncertainties, taken together, our sedimentation and cross-linking experiments suggest that hantavirus nucleocapsid proteins have a tendency to trimerize and form trimers in infected cells and virus particles.

What N protein domains associate with each other to facilitate oligomerization? We employed a modification of the yeast two-hybrid system (6) to address this question. Following previously established methods (2, 6, 12, 16), we constructed an amino-terminal fusion of the SNV N protein coding region to the herpesvirus VP16 activator domain to make the vector VP16-N. We also constructed a series of N protein fusions to the DNA binding domain of LexA (Fig. 4). As diagrammed, in addition to the negative control construct Lex-EBfill and the full-length fusion construct Lex-N, three C-terminal truncation plasmids—Lex-N1-357, Lex-N1-171, and Lex-N1-172—were created. N-terminal truncation constructs were Lex-N172-428 and Lex-N172-357, which also carried a deletion of the C-terminal 71 codons. Internal deletion constructs were Lex-NΔ157-372, Lex-NΔ40-195, and Lex-NΔ40-214, while Lex-Nins156, Lex-Nins268, and Lex-Nins372 carried linker insertion mutations. To ensure that constructs were expressed appropriately, proteins from transformed yeast cells were immunodetected by Western blotting using an anti-LexA antibody (sc-7544 [Santa Cruz Biotech] at a 1:1,500 dilution). In all cases, correctly sized LexA proteins were detected, whereas untransformed control cells yielded no detectable signal (data not shown).

Our approach to two-hybrid analysis of SNV N protein interactions was to coexpress Lex-N variants (Fig. 4) with VP16-N in *Saccharomyces cerevisiae* strain L40 (2, 12). As with other two-hybrid analyses (2, 6, 12, 16), interaction of N protein moieties on different fusion partners was expected to induce β-galactosidase expression, which was measured by a β-galactosidase filter assay of at least four independent cotransformant colonies. As shown in Fig. 5, activity levels from VP16-N plus Lex-N cotransformants (N) consistently yielded activity levels four- to fivefold higher than those of the negative control VP16-N plus Lex-EBfill (EBfill). The VP16-N plus Lex-N levels were normalized to 100% and were 20 times greater than Lex-N single transformant signals (Fig. 5). These results indicate that N protein association was readily detectable with this genetic system.

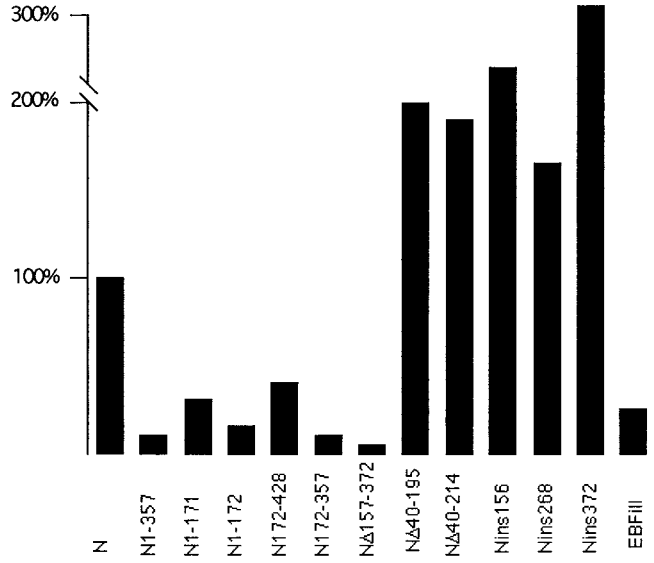

FIG. 5. Genetic analysis of N protein interactions. Protein-protein interactions between VP16-N proteins and the indicated Lex-N fusion proteins were monitored by quantitation of β-galactosidase activities. To do so, a yeast (*S. cerevisiae*) L40 (2, 12) strain expressing VP16-N was constructed by lithium acetate (2, 12) transformation and selection on Leu^- plates. Subsequent transformation of Lex constructs into L40 and L40 VP16-N parental strains used Trp^- or Trp^- Leu^- selections, respectively. For assays, parental and transformant yeast colonies were transferred with toothpicks onto nitrocellulose filter squares, which were placed into precooled aluminum boats floating on liquid nitrogen for 30 s and then submerged in liquid nitrogen for 5 s. Frozen cells on filters were thawed at room temperature, after which filters were transferred onto Whatman papers in petri dishes impregnated with Z buffer (100 mM sodium phosphate, pH 7.0, 10 mM KCl, 1 mM $MgSO_4$) containing 0.25 mg of X-Gal (5-bromo-4-chloro-3-indolyl-β-D-galactopyranoside)/ml. Experimental, positive, and negative control filters were incubated at 30°C for 16 h to allow for color development, after which cells on filters were dried at room temperature. For quantitation, dried filter images were scanned at 150 dpi with a Hewlett-Packard Scan Jet IIc scanner and densitometrically quantitated using the gel plot program of NIH Image 1.62. Activity levels correspond to those from yeast strains doubly transformed with VP16-N and the indicated Lex-N construct and were normalized to those of the average of L40 VP16-N Lex-N (N) double transformants. Values are derived from the number (n) of independent β-galactosidase measurements listed below, and background activity levels (b) for each Lex-N construct were determined from a minimum of four measurements in transformed cells lacking the VP16-N construct and are also listed: Lex-N, $n = 33$, $b = 5\%$; Lex-N1-357, $n = 17$, $b = 19\%$; Lex-N1-171, $n = 24$, $b =$ not done; Lex-N1-172, $n = 6$, $b = 17\%$; Lex-N172-428, $n = 16$, $b = 16\%$; Lex-N172-357, $n = 22$, $b = 12\%$; Lex-NΔ157-372, $n = 8$, $b = 12\%$; Lex-NΔ40-195, $n = 10$, $b = 13\%$; Lex-NΔ40-215, $n = 4$, $b = 22\%$; Lex-Nins156, $n = 4$, $b = 20\%$; Lex-Nins268, $n = 6$, $b = 16\%$; Lex-Nins372, $n = 3$, $b = 42\%$; Lex-EBfill, $n = 4$, $b = 13\%$.

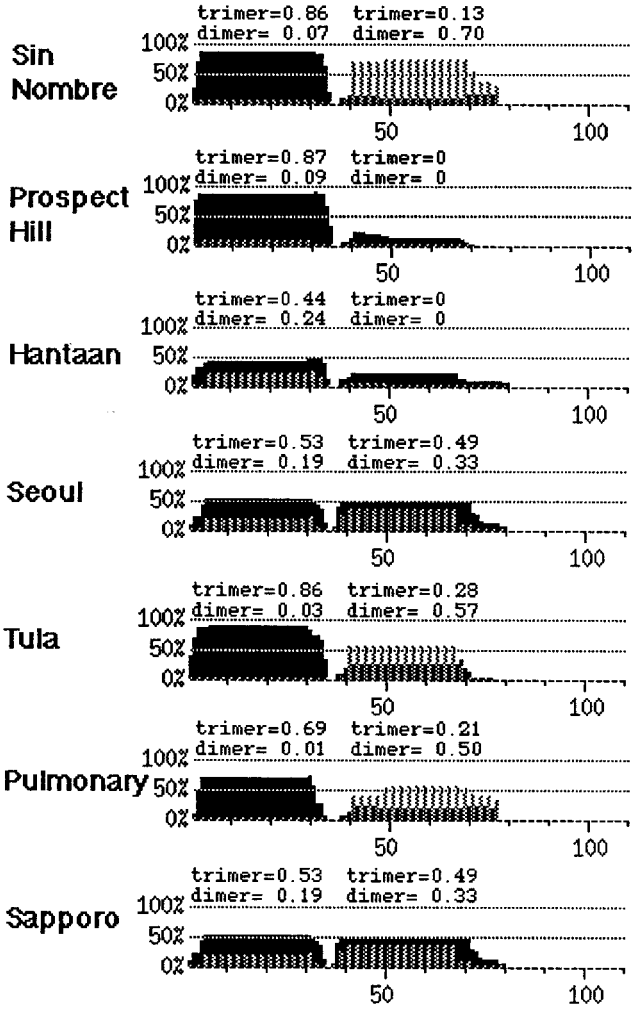

FIG. 6. Prediction of N protein coiled-coil domains. The N protein sequences of Sin Nombre, Prospect Hill, Hantaan, Seoul, Tula, Pulmonary, and Sapporo strains of hantavirus were subjected to the MultiCoil (29) parallel coiled-coil prediction algorithm, using a 0.5 cutoff for the maximum scoring residue. The graphs show the calculated probabilities (y axis) for trimeric (solid bars) and dimeric (hatched bars) coiled coils versus N protein residues 1 to 110 (x axis). Note that MultiCoil probabilities for coiled coils in residues 111 to 428 were below threshold values. As shown, two possible coiled coils are predicted, at residues 1 to 34 and 38 to 80. For each sequence, predicted trimer and dimer probabilities for the 1 to 34 and 38 to 80 coiled coils are provided at the top of each graph. Probabilities of 0 indicate that no residue in a region scored above the 0.5 cutoff value.

Identification of N protein interaction domains was undertaken via analysis of Lex-N deletion and insertion mutants (Fig. 4). Perhaps not surprisingly, no single linker insertion mutation resulted in a significant diminution of β-galactosidase activity signals (Lex-Nins156, Lex-Nins268, Lex-Nins372). In contrast, several deletion mutations apparently reduced or eliminated two-hybrid signals. In particular, β-galactosidase signals from constructs carrying C-terminal truncations (Lex-N1-357, Lex-N1-171, Lex-N1-172, and Lex-N172-357) were less than one-third of wild-type (wt) Lex-N levels. Similarly, Lex-N172-428, the amino-terminal deletion construct, showed reduced activity levels, although the effects were not as pronounced as those of C-terminal truncation mutants.

The above results implied that coassociation of SNV N proteins depended on sequences near their N and C termini. The importance of N protein central domains was underscored by the low signal obtained with the Lex-NΔ157-372 construct. However, two deletion constructs, Lex-NΔ40-195 and Lex-NΔ40-215, yielded notably high two-hybrid signals: their β-galactosidase signals were twice those of the wt construct and greater than five times those of any other deletion construct. Comparison with Lex-N172-428, which yielded essentially a

negative two-hybrid result, suggests that retention of the amino-terminal 39 residues on the Lex-NΔ40-195 and Lex-NΔ40-215 proteins greatly boosted their abilities to associate with VP16-N proteins. Thus, the hantavirus N interaction domain may be confined to the C-terminal half of the protein plus a short N-terminal segment.

Although our computer homology searches of full-length hantavirus N protein sequences generally have yielded homologies only to the 100-plus N protein-related sequences in the protein databases, searches with fragments of the N protein sequence proved potentially informative with regard to oligomerization. In particular, database queries employing N protein N-terminal sequences yielded homologies (27 to 33% identities) to coiled-coil proteins. Based on these results, we subjected N protein sequences of Sin Nombre, Prospect Hill, Hantaan, Seoul, Tula, Pulmonary, and Sapporo strains of hantavirus (1, 3, 13, 20, 24, 26, 28) to analysis by MultiCoil, the coiled-coil prediction algorithm of Wolf et al. (29). With all seven sequences, no coiled-coil regions were predicted in C-terminal 350 N protein residues, but coiled-coil structures were predicted in the amino-terminal domains (Fig. 6). Specifically, two sequence stretches, residues 1 to 34 and 38 to 80, were predicted to form coiled coils. Predictions for the sequence at residues 38 to 80 were somewhat variable, with two hantavirus strains (PHV and Hantaan) receiving scores below the 50% probability cutoff (29) and others scoring in the 70 to 80% probability range, with no clear distinction between dimeric and trimeric coils (Fig. 6). In contrast, residues 1 to 34 from all seven hantavirus strains were strongly predicted to form parallel (29) trimeric coiled coils. Since this region corresponds to the N protein N-terminal domain implicated as an interaction region in two-hybrid screens (Fig. 5), it seems likely that N protein trimerization observed in vivo involves these residues. Efforts are under way to test these structural predictions.

Ayna Alfadhli and Zac Love contributed equally to the completion of this work.

We are grateful to Stuart Nichol for antibodies to the SNV N protein and its molecular clone, to Thomas Ksiazek for twice sending us PHV stocks, and to Connie Schmaljohn for anti-hantavirus sera and expression vectors. Mike Marusich's help in the production of necessary immunological reagents for our studies is appreciated greatly. Stanley Hollenberg's yeast two-hybrid system expertise was invaluable, and we are thankful to lab members Sonya Karanjia, Jason McDermott, Keith Mayo, and Eric Steele for advice and assistance.

This research could not have been accomplished without the support of the American Heart Association (grant number 9950069N).

REFERENCES

1. **Arikawa, J., H. Lapenotiere, L. Iacono-Connors, M. Wang, and C. Schmaljohn.** 1990. Coding properties of the S and the M genome segments of Sapporo rat virus: comparison to other causative agents of hemorrhagic fever with renal syndrome. Virology **176:**114–125.
2. **Chen, C.-M. A., N. Kraut, M. Groudine, and H. Weintraub.** 1996. I-mf, a novel myogenic repressor interacts with members of the MyoD family. Cell **86:**731–741.
3. **Chizhikov, S., C. Spiropoulou, S. Morzunov, M. Monroe, C. Peters, and S. Nichol.** 1995. Complete genetic characterization and analysis of isolation of Sin Nombre virus. J. Virol. **69:**8132–8136.
4. **Dunn, E., D. Pritlove, H. Jin, and R. Elliott.** 1995. Transcription of a recombinant bunyavirus RNA template by transiently expressed bunyavirus proteins. Virology **211:**133–143.
5. **Feldmann, H., A. Sanchez, S. Morzunov, C. Spriopoulou, P. Rollin, T. Ksiazek, C. Peters, and S. Nichol.** 1993. Utilization of autopsy RNA for the synthesis of the nucleocapsid antigen of a newly recognized virus associated with hantavirus pulmonary syndrome. Virus Res. **30:**351–367.
6. **Fields, S., and O. Song.** 1989. A novel genetic system to detect protein-protein interactions. Nature **340:**245–246.
7. **Gavrilovskaya, I., E. Brown, M. Ginsberg, and E. Mackow.** 1999. Cellular entry of hantaviruses which cause hemorrhagic fever with renal syndrome is mediated by B3 integrins. J. Virol. **73:**3951–3959.
8. **Gavrilovskaya, I., M. Shepley, R. Shaw, M. Ginsberg, and E. Mackow.** 1998. B2 integrins mediate the cellular entry of hantaviruses that cause respiratory failure. Proc. Natl. Acad. Sci. USA **95:**7074–7079.
9. **Goldsmith, C., L. Elliott, C. Peters, and S. Zaki.** 1995. Ultrastructural characteristics of Sin Nombre virus, causative agent of hantavirus pulmonary syndrome. Arch. Virol. **140:**2107–2122.
10. **Gott, P., R. Stohwasser, P. Schnitzler, G. Darai, and E. Bautz.** 1993. RNA binding of recombinant nucleocapsid proteins of hantaviruses. Virology **194:** 332–337.
11. **Hansen, M., and E. Barklis.** 1995. Structural interactions between retroviral Gag proteins examined by cysteine cross-linking. J. Virol. **69:**1150–1159.
12. **Hollenberg, S., R. Sternglanz, P. Cheng, and H. Weintraub.** 1995. Identification of a new family of tissue-specific basic helix-loop-helix proteins with a two-hybrid system. Mol. Cell. Biol. **15:**3818–3822.
13. **Huang, C., W. Campbell, R. Means, and D. Ackman.** 1996. Hantavirus S RNA sequence from a fatal case of HPS in New York. J. Med. Virol. **50:**5–8.
14. **Hutchinson, K., C. Peters, and S. Nichol.** 1996. Sin Nombre virus mRNA synthesis. Virology **224:**139–149.
15. **Lindwall, G., M. F. Chau, S. Gardner, and L. A. Kohlstaedt.** 2000. A sparse matrix approach to the solubilization of overexpressed proteins. Protein Eng. **13:**67–71.
16. **Luban, J., K. Alin, K. Bossolt, T. Humaran, and S. Goff.** 1992. Genetic assay for multimerization of retroviral Gag polyproteins. J. Virol. **66:**5157–5160.
17. **McDermott, J., L. Farrell, R. Ross, and E. Barklis.** 1996. Structural analysis of human immunodeficiency virus type 1 Gag protein interactions using cysteine-specific reagents. J. Virol. **70:**5106–5114.
18. **McDermott, J., S. Karanjia, Z. Love, and E. Barklis.** 2000. Crosslink analysis of N-terminal, C-terminal, and N/B determining regions of the Moloney murine leukemia virus capsid protein. Virology **269:**190–200.
19. **Moriwawa, Y., D. Hockley, M. Nermut, and I. Jones.** 2000. Roles of matrix, p2, and N-terminal myristoylation in human immunodeficiency virus type 1 Gag assembly. J. Virol. **74:**16–23.
20. **Parrington, M., and C. Y. Kang.** 1990. Nucleotide sequence analysis of the S genomic segment of Prospect Hill virus: comparison with the prototype hantavirus. Virology **175:**167–175.
21. **Persson, R., and R. Petterson.** 1991. Formation and intracellular transport of a heterodimeric viral spike protein complex. J. Cell Biol. **112:**257–266.
22. **Ravkov, E., S. Nichol, and R. Compans.** 1997. Polarized entry and release in epithelial cells of Black Creek Canal virus, a new world hantavirus. J. Virol. **71:**1147–1154.
23. **Ravkov, E., S. Nichol, C. Peters, and R. Compans.** 1998. Role of actin microfilaments in Black Creek Canal virus morphogenesis. J. Virol. **72:**2865–2870.
24. **Schmaljohn, C.** 1996. Molecular biology of hantaviruses, p. 63–90. *In* R. Elliott (ed.), The Bunyaviridae. Plenum Press, New York, N.Y.
25. **Schmaljohn, C., and B. Hjelle.** 1997. Hantaviruses: a global disease problem. Emerg. Infect. Dis. **3:**95–104.
26. **Schmaljohn, C., G. Jennings, J. Hay, and J. Dalrymple.** 1986. Coding strategy of the S genome segment of Hantaan virus. Virology **155:**633–643.
27. **Severson, W., L. Partin, C. Schmaljohn, and C. Jonsson.** 1999. Characterization of the Hantaan nucleocapsid protein-ribonucleic acid interaction. J. Biol. Chem. **274:**33732–33739.
28. **Sibold, C., H. Meisel, D. Kruger, M. Labuda, J. Lysy, O. Kozuch, M. Pejcoch, A. Vaheri, and A. Plyusnin.** 1999. Recombination in Tula hantavirus evolution: analysis of genetic lineages from Slovakia. J. Virol. **73:**667–673.
29. **Wolf, E., P. Kim, and B. Berger.** 1997. MultiCoil: a program for predicting two- and three-stranded coiled coils. Protein Sci. **6:**1179–1189.